ACTA GEOLOGICAHISPANICA, v. 36 (2001), nº 3-4, p. 245-266

Paleo and historical seismicity in Mallorca (Baleares, Spain) a preliminary approach

Paleosismicidad y sismicidad histórica en Mallorca (Baleares, España): una aproximación preliminar

P.G. SILVA[1], F.M. GONZÁLEZ HERNÁNDEZ[2], J.L. GOY[2], C. ZAZO[3] and P. CARRASCO[4]

(1) Depto. Geología, Universidad de Salamanca, Escuela Politécnica Superior de Ávila. 05003 Avila (Spain). pgsilva@gugu.usal.es

(2). Depto. Geología, Universidad de Salamanca, Fac. Ciencias. 37008 Salamanca (Spain)

(3) Depto. Geología, Museo Nac. CC. Naturales (CSIC), Gutiérrez Abascal, 2. 28006 Madrid (Spain)

(4) Depto. Ingeniería del Terreno, Universidad de Salamanca, Escuela Politécnica Superior de Ávila. 05003 Avila (Spain)

ABSTRACT

The island of Mallorca is subject to low seismic activity. The instrumental record shows that current seismicity is surficial (<10 km depth) and low in magnitude (mb<4). Both historical and geological records display the occurrence of strong events, e.g. the 1851 Palma earthquake (VIII, MSK intensity). Data on this destructive event indicate that this was a seven month long seismic sequence, with two strong events, causing severe damage and collapse of buildings along Palma bay in addition to moderate ground collapses in the macroseismal zone. The earthquake epicenter was situated between Sa Cabaneta and Sta. Eugènia. This earthquake can be correlated with the trace of the Sencelles fault, the main extensional structure of the island on the surface. The geological and geophysical analyses of recent surface faulting features at the Portol doline (reverse surface faulting) and on the Sta. Eugènia segment of the Sencelles fault (bedrock fault scarp) suggest recurrent large prehistoric events. Preliminary data show minimum vertical offsets of 2.56 m at the Portol doline and offsets of 3.50 m at the Sta. Eugènia bedrock fault scarp. These offsets were accumulated in recent times (Holocene?). Displacements per event can be initially estimated as mean values of 0.88 to 0.40 m in both places, but larger offsets of a maximum of 1.68 m can also be inferred. Specific dendrochronologic, lichenometric, and weathering analyses to assess true single-event slip values, and their time-bracketing will be necessary. The interpretation of these displacement events in terms of earthquake magnitude is not straightforward because of the apparent subordinate nature of the ground rupture at the Portol doline and the possible influence of salt tectonics in both places. To address these issues, a fault-trench was planned along the Sencelles fault within the framework of a new research project. The Spanish seismic code (NCS94) assigns an expected maximum ground acceleration of 0.04 g for a 500 year return period to the area. In the light of our data these values are underestimated. The historical and geological records indicate the occurrence of historical VII to VIII MSK, and stronger prehistoric events. Peak ground horizontal accelerations of up to 0.10 g could be expected during modern earthquakes.

Keywords: Paleoseismicity. Seismicity. Surface faulting. Ground failures. Mallorca. Spain.

RESUMEN

La isla de Mallorca presenta una actividad sísmica baja. El registro instrumental muestra que la sismicidad actual es superficial (<10 km de profundidad) y de baja magnitud (mb<4). Tanto el registro histórico como el geológico presentan eventos fuertes, p. ej. el terremoto de Palma de 1851 (intensidad MSK, VIII). Los datos sobre este evento destructivo indican que se trató de una secuencia sísmica de siete meses de duración, con dos eventos fuertes que causaron importantes daños y el hundimiento de edificios en la bahía de Palma, así como moderados colapsos del suelo en la zona macrosísmica. El epicentro se situó entre Sa Cabaneta y Sta. Eugènia. Este terremoto puede asociarse a la traza de la falla de Sencelles, la mayor estructura extensional de la isla en superficie. El análisis geológico y geofísico de las fallas superficiales recientes en la dolina de Portol (falla inversa en superficie) y en el segmento de Sta. Eugènia de la falla de Sencelles (escarpe de falla) sugiere la ocurrencia de grandes eventos prehistóricos recurrentes. Los datos preliminares indican desplazamientos verticales mínimos de 2,56 m en la dolina de Portol y de 3,50 m en el escarpe de falla de Sta. Eugènia. Estos desplazamientos se han acumulado en tiempos recientes (¿Holoceno?). En ambas localidades pueden estimarse desplazamientos medios por evento comprendidos entre 0,88 y 0,40 m, aunque se han podido inferir desplazamientos de hasta 1,68 m. Para delimitar eventos individuales y acotarlos temporalmente serán necesarios análisis dendrocronológicos, liquenométricos y de meteorización. La interpretación de estos eventos de desplazamiento en términos de magnitudes de terremotos no es simple debido a la subordinación de la ruptura a la dolina de Portol y a la posible influencia de la tectónica salina en ambas localidades. Para abordar estos problemas se ha planeado la realización de una trinchera a través de la falla de Sencelles, en el marco de un nuevo proyecto de investigación. El código sísmico español (NCS94) asigna una aceleración máxima del suelo de 0,04 g para un período de retorno de 500 años en este área. A la luz de nuestros datos estos valores están infraestimados. Tanto los registros históricos como los geológicos indican la ocurrencia de terremotos históricos de I (MSK) VII o VIII, y sismos prehistóricos más fuertes. Pueden esperarse aceleraciones horizontales del suelo de hasta 0,10 g durante terremotos futuros.

Palabras clave: Paleosismicidad. Sismicidad. Falla superficial. Mallorca. España.

INTRODUCTION

This paper describes the most recent paleoseismic research carried out in Mallorca. Our investigation commenced in 1995 within the framework of different research projects of the University of Salamanca and the Museo Nacional de Ciencias Naturales (CSIC). Most research has been focussed on the identification of recent faulting events obtained from geomorphologic and stratigraphic evidence along the complex SE and SW borders of the Inca basin and specific zones around the Palma bay basin. A detailed study of the last destructive earthquake felt on the island (the 1851 Palma earthquake: VIII MSK) was undertaken to correlate the deformations observed with this seismic event (Fig. 1). This event seems to be genetically related to the Sencelles fault in the SW corner of the Inca basin. Most of the investigation was carried out by direct observation in artificial trenches and selected natural outcrops, and by using specific high-resolution geophysical prospecting. A fault-trenching project in the westernmost sector of the Sencelles fault is in preparation.

GEOLOGICAL AND STRUCTURAL SETTING

Mallorca constitutes the most important emerged segment of the Balearic promontory, which forms the northeastern prolongation of the external zones of the Betic Cordillera (east Spain) into the Mediterranean sea (Fontboté et al., 1990). The overall structure of the island comprises a set of NE-SW trending basins and ranges which were formed during a period of tectonic extension that has been active since the late Miocene (Alvaro, 1987, Benedicto et al., 1993). The structure of the ranges is compressional. These ranges were made up of a pile of thrust sheets no more than a few kilometers long and hundreds of meters thick during the Paleogene-lower Miocene betic nappe emplacement (Gelabert et al., 1992; Sábat et al., 1988). The Serra de Tramuntana in the Northwest and the Serres de Llevant in the Southeast constitute the main reliefs. In contrast, the basins are half-grabens along the detached horizons of old NE-SW thrust planes, controlled by a broad NW-SE trending extensional stress field which has been active until recent Quaternary times (Alvaro et al., 1984; Benedicto et al., 1993). The most important set of basins were formed at the foot of the Serra de Tramuntana, generating a Neogene-Quaternary sedimentary trough. This trough is more than 80 km long, 10-6 km wide and more than 0.7 km deep, and is bounded on the SE by the Sencelles fault, the main NE-SW normal fault of the island. The Quaternary sedimentary basins of Palma bay, Inca, and Alcúdia (Fig. 1) are currently related to this fault.

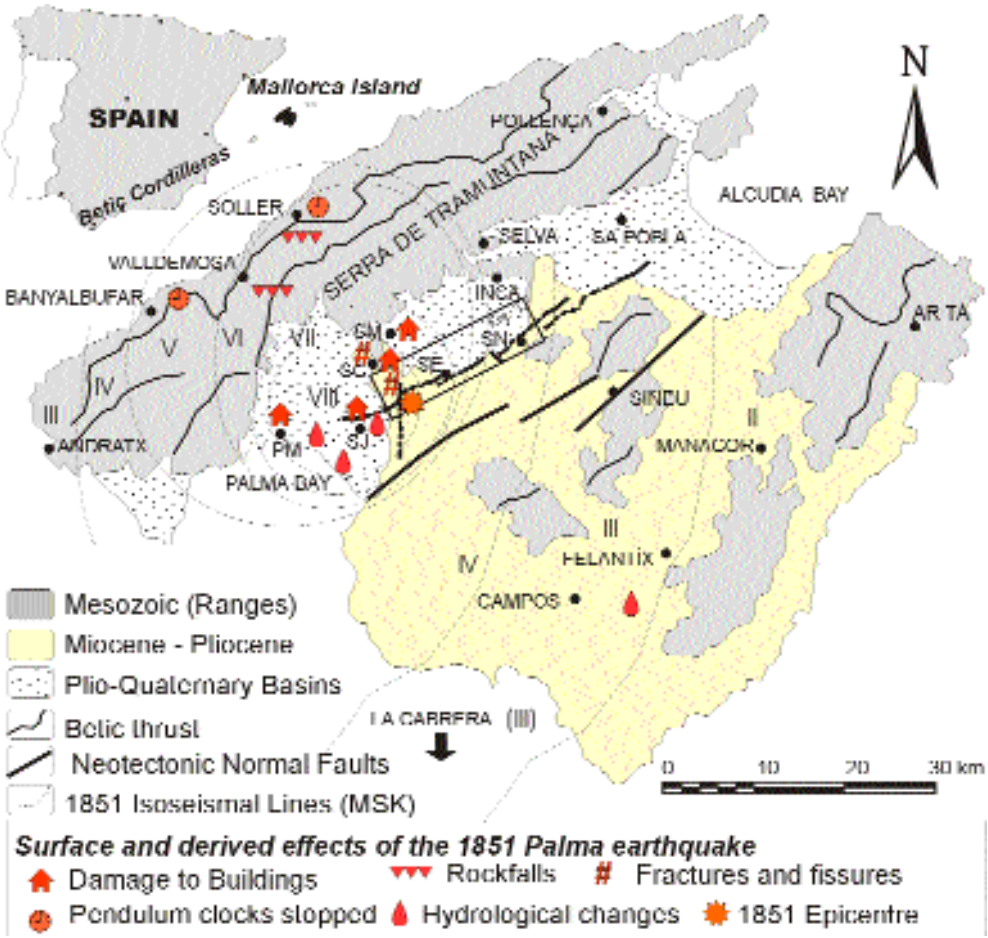

Figure 1. Geological and structural framework of Mallorca, showing the location of the Sencelles fault, main ground-derived effects and isoseismal map of the 1851 Palma earthquake. Studied sites in relation to the 1851 Palma earthquake epicentral location. Abbreviated locations: PM (Palma de Mallorca); SJ (Sant Jordi); SC (Sa Cabaneta); SM (Sta. Maria del Camí); SE (Sta. Eugènia). Box indicates the mapped zone in Fig. 3.

Figura 1. Marco geológico y estructural de Mallorca con la situación de la falla de Sencelles, los principales efectos del terremoto de Palma (1851) y mapa de isosistas. Localidades estudiadas en relación con la situación del epicentro del terremoto de Palma de 1851. Localidades abreviadas: PM (Palma de Mallorca); SJ (Sant Jordi); SC (Sa Cabaneta); SM (Sta. Maria del Camí); SE (Sta. Eugènia). El recuadro indica la zona cartografiada de la Fig. 3.

The most developed recent extensional structures are located along the Sencelles fault, where a well defined bedrock fault scarp cuts through the Plio-Quaternary calcarenites of the St. Jordi Fm. and through the oldest Serravallian deposits of the Margas de Pina Fm. (Pomar et al., 1983; Simó and Ramón, 1986). This NW dipping structure constitutes the southern border of the Inca basin and has been active since at least Serravallian times (Simó and Ramón, 1986), resulting in the formation of the aforementioned sedimentary trough. Models based on gravity surveys and onshore seismic reflection profiles indicate that this major fault has an accumulated throw of about 750 m (Benedicto et al., 1993; Gelabert, 1998). To the South lies the other main extensional structure of the island, the Sineu-Algaida fault (Del Olmo and Alvaro, 1984), which runs obliquely across the northern sector of the Serres de Llevant (Sábat et al., 1988).

Despite the prevailing NW-SE extensional setting, anomalous NW-SE trending "compressive" features have been reported in the complex antiform threshold separating the Palma bay and Inca basins (Benedicto et al., 1993; Del Olmo et al., 1991, Goy et al., 1991). A variety of Mesozoic materials crop out in the central part

of these complex structures. Gypsiferous Serravallian materials (Margas de Pina Fm.) display an elliptical-shaped antiform. Most of these structures, including recent surface reverse faults, have been related to roll-overs along the main extensional faults and/or to lateral ramps of the inherited betic thrust planes (Dañobeitia et al., 1992; Silva et al., 1997; Silva et al., 1999). The formation of these structures could have been assisted by near-surface diapiric processes (Silva et al., 2000). This view is also supported by a strong gravity anomaly of more than -13 mgal centered in the SW corner of the Inca basin (Benedicto et al., 1993), which includes the aforementioned antiform-like structures.

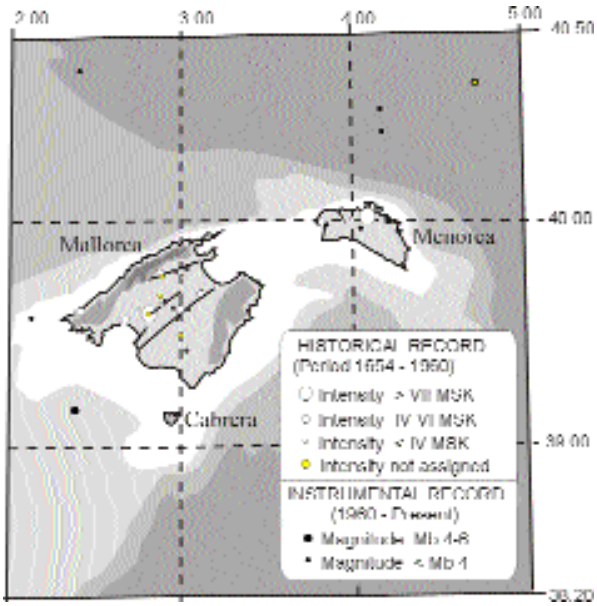

Figure 2. Seismicity in Mallorca and Menorca (2.00 - 5.00ºE and 38.20 - 40.50ºN). Redrawn from the IGN Seismic Data Bank (UTM Projection; H30). Data petition nº 96/0001 (period 800 BC - 1996 AD), updated to 1999 by on-line seismic data on: www/geo.ign.es.

Figura 2. Sismicidad de Mallorca y Menorca (2.00 - 5.00ºE y 38.20 - 40.50ºN). Redibujado del banco de datos sísmicos del IGN (proyección UTM; H30). Petición de datos nº 96/0001) (período 800 BC - 1996 AD), actualizado hasta 1999 con datos sísmicos tomados on-line de: www/geo.ign.es.

SEISMICITY AND SEISMOTECTONICS

Seismicity in Mallorca (Fig. 2) is low. Only 21 events were included in the Spanish seismic data bank elaborated by the IGN for the period 1654-1996 (IGN, 1996; Table 1). There were no data prior to 1654. Only the seven last seismic events since 1970 offer reliable focal parameters. This instrumental record shows shallow (<10 km depth) and low magnitude (< 3.5 mb) seismicity in the inland sector. Moderate earthquakes of up to 4.3 mb occurred in neighboring offshore localities in the Valencia trough.

Despite the low level of seismic activity in recent decades, some large historical earthquakes have occurred, inducing strong ground shaking inland. The first documented events were felt in the northern sector of the island along the Serra de Tramuntana with maximum intensities of VII MSK (IGN, 1996) and only 61 years apart (1660-1721: Table 1). After an interval of 130 years, on 15 May 1851, the strongest earthquake to strike the island had a maximum intensity of VIII MSK (IGN, 1996). Some authors (Del Olmo and Alvaro, 1984; Silva et al., 1999) attribute this event to the Sencelles fault. Seismic activity during the 20th century was lower than that of the 19th century. Discrete events occurred in two well defined periods: (A) 1919-1923 and (B) 1995-1996. The first period (A), 68 years after the 1851 event, was initiated by the V MSK Montuiri event (Mezcua, 1982), followed by two IV MSK events at Sencelles and Sa Pobla, and terminated by a III MSK event at Sant Joan

Table 1. Seismic events and available seismological parameters listed in the Spanish seismic data bank of the IGN. Data Petition nº 96/0001 (period 800 BC - 1996 AD), updated to 1999 by on-line seismic data on: www/geo.ign.es. (see Fig. 2). ®: Main documented aftershocks. (*) Artificially located macroseismal epicenters. White and shaded boxes highlight the sequence of the main seismic periods in Mallorca. Lower graph illustrates the time-distribution of seismic activity on the island. Arrows show the specific elapsed times between strong earthquakes (stars) and those related to the Sencelles fault (circles).

Tabla 1. Eventos sísmicos y parámetros sísmicos disponibles en el banco de datos sísmicos español del IGN. Petición de datos nº 96/0001 (período 800 BC-1996 AD), actualizado hasta 1999 con datos tomados on-line en : www/geo.ign.es (véase Fig. 2). ®: Principales réplicas documentadas. (*) Epicentros macrosísmicos situados artificialmente. Recuadros blancos y sombreados resaltan la secuencia de los principales períodos sísmicos en la isla de Mallorca. El gráfico de la parte baja ilustra la distribución temporal de la actividad sísmica de la isla. Las flechas muestran el tiempo transcurrido entre los terremotos fuertes (estrellas) y los relacionados con la falla de Sencelles (círculos).

DATE	LONGITUDE	LATITUDE	Depth (km)	EH (km)	EZ (km)	INT MSK	MAG mb	LOCATION	OBSERVATIONS
1660-10-20	02.24.0E	39.36.0N				VII		W PALMA M	Noticeably felt at Palma bay and western coast of the island *
1721-03-24	02.54.0E	39.48.0E				VII		SELVA	Noticeably felt at Alcudia bay and Inca basin (hydrological changes)
1763-07-02	02.45.0E	39.38.0E						STA. MARIA CAMÍ	No relevant data *
1764--05-26	03.00.0E	39.36.0N						**SENCELLES**	
1783-03-14	02.54.0E	39.42.0N						INCA	
1827-00-00	03.00.0E	39-38.0N				VI		SINEU	Felt in the central sector of the island
1835-06-16	02.24.0E	39.36.0N				V		PALMA M	Felt all around Palma bay *
1851-05-15	02.48.0E	39.36.0N				VIII		**SE ST EUGÈNIA**	1851 Palma Seismic sequence Seven months long; 2major events
1851-06-07	02.48.0E	39.36.0N				VI ®		**SE ST EUGÈNIA**	
1852-08-31	02.48.0E	39.36.0N				V		**SE ST EUGÈNIA**	Panic at Palma, Felt at Palma bay
1859-03-18	02.10.0E	39.35.0N						PALMA M	No relevant data*
1860-03-18	02.10.0E	39.35.0N				III		PALMA M	
1860-03-26	02.10.0E	39.35.0N				®		PALMA M	
1863-07-00	02.24.0E	39.36.0N						PALMA M	
1876-07-25	03.00.0E	39.30.0N						PALMA M	Not catalogued by Galbis, but listed in the present IGN data bank (No data)
1887-05-06	02.38.0E	39.35.0N				III		PALMA M	No relevant data *
1887-09-07	02.38.0E	39.35.0N				IV		PALMA M	Felt at Palma bay *
1919-10-08	02.59.0E	39.35.0N				V		MONTUIRI	Felt in the central sector of the island.
1921-10-22	02.54.0E	39.39.0N				IV		**SENCELLES**	Felt in the southern sector Inca basin
1923-04-09	03.01.0E	39.46.0N				IV		SA POBLA	Felt at Alcudia bay
1923-07-04	03.02.0E	39.36.0N				III		SAN JUAN	No relevant data
1923-12-14	03.17.0E	40.50.0N				III		MEDITERRÁNEO	Offshore event: Felt at Alcudia bay
1925-08-20	02-10.0E	39.35.0N					4.3	MEDITERRÁNEO	Offshore event: Not felt
1971-04-30	01.05.1E	39.49.5N	5	29	28		3.4	MEDITERRÁNEO	Offshore events to the WSW of Mallorca (not included in Fig. 2)
1973-06-01	00.51.1E	39.04.6N	5	51	55		3.7	MEDITERRÁNEO	
1978-07-28	02-22.8E	39.10.2N	5	8	10	III	4.2	MEDITERRÁNEO	Offshore event: Felt at Palma bay
1995-03-01	03.02.0E	39.26.0N	4	1	--	II-III	2.6	CAMPOS	Felt in the central sector of the island (no relevant data)
1996-04-01	03.03.5E	39.37.5N	3	6	4	II-III	3.3	SINEU	
1996-04-02	03.01,2E	39.48.0N	2	1	3	II	3.0	**SA POBLA**	Alcudia bay – SE sector Inca basin
1996-04-09	02.55.6E	39.38.8N	10	3	2	II-III	2.8	**SENCELLES**	Southern sector Inca basin

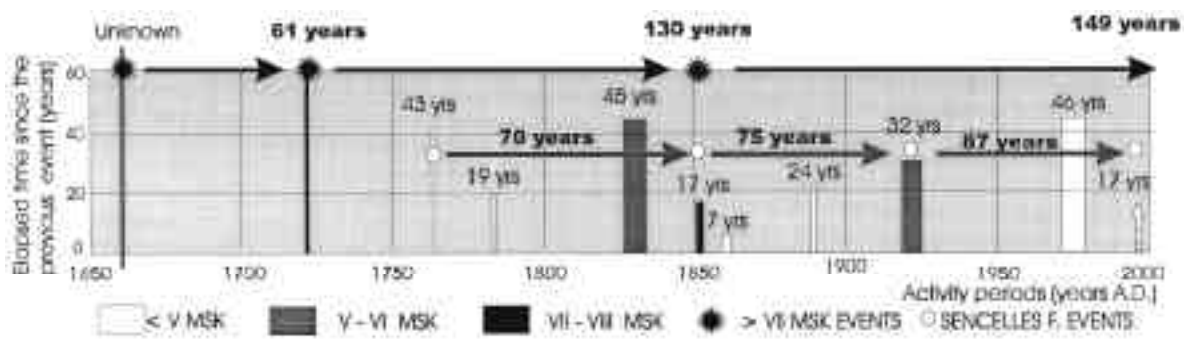

(Table 1). During the second period (B) only II-III MSK intensities were produced by 3.3 to 2.6 mb shallow earthquakes at recurrent sites such as Campos, Sineu, Sencelles and Sa Pobla, the three last within a period of 8 days, in March 1996 (Table 1).

Not all the recorded events can be correlated with the Sencelles fault. Aside from the 1851 seismic sequence, only four other events can be related to this structure taking into account focal parameter errors EH and EZ. This is the case of the two last seismic events in 1996, and also of the two historical events in 1764 and 1921 (Table 1 and Fig. 2). Bearing these events in mind, broadly homogeneous recurrence intervals of 70-90 years characterize the activity of the Sencelles fault (Table 1). As in the case of the 1851 event, other historical events allegedly located in Palma, could also have been produced by this fault. In this regard, once all the catalog events are considered, the release of the seismic energy of the island seems to have been dominated by clusters of earthquakes of recurrence intervals of 40-50 and of 17-19 yr.

Given the time elapsed (149 years) since the last destructive earthquake (1851), it is reasonable to assume that the Sencelles fault has accumulated sufficient elastic energy to generate a new VIII MSK seismic event. Therefore, an investigation of the seismicity that occurred prior to the 1851 earthquake and a study of the characteristics of the 1851 event could yield insights into the seismic behavior of the suspected seismic sources. This would contribute to a more reliable basis for assessing the seismic hazard of the island.

Table 2. List of the seismic sequence related to the 1851 Palma earthquake. Data from Galbis (1935); IGN (1996) and contemporary reports of Bouvy (1851; 1853) and Pujó (1851).

Tabla 2. Lista de la secuencia sísmica relacionada con el terremoto de Palma de 1851. Datos de Galbis (1935); IGN (1996) y relatos contemporáneos de Bouvy (1851; 1853) y Pujó (1851).

Date	Time	Description	Intensity (MSK)
1851-05-15	01:47:00	Main shock (see text): severe damage to buildings and moderate ground collapses	VIII (IGN)
1851-05-15	05:00:00	Noticeably felt, strong seismic tremor	> VI
1851-05-18	20:30:00	Only felt by some people	III-II
1851-05-21	14:30:00	Only felt, seismic tremor.	III-II
1851-05-22	04:00:00	Noticeably, panic at Palma	V-IV
1851-06-07	18:00:00	Panic at Palma and total destruction of St. Marçal church at Marratxí (Sa Cabaneta)	VI (IGN)
1851-06-28	00:00:00	Light shaking	
1851-08-28	00:00:00	Only felt by some people	
1851-08-31	00:00:00	Only felt by some people	
1851-09-16	00:00:00	Only felt by some people	
1851-09-17	00:00:00	Only felt by some people	< III
1851-09-28	00:00:00	Only felt by some people	
1851-11-09	00:00:00	Only felt by some people	
1851-12-22	00:00:00	Only felt by some people	
		Only felt by some people	
1852-05-11	00:00:00	Light shaking felt at Palma bay	III
1852-06-04	00:00:00	Only felt by some people	II-III
1852-06-10	00:00:00	Noticeably felt	III
1852-08-31	00:00:00	Strong shaking at Palma. Panic. Most people leave houses	V (IGN)

THE 1851 PALMA EARTHQUAKE

On the basis of different catalogs (Galbis, 1932; IGN, 1996) and contemporary reports (Bouvy, 1851; 1853; Pujó, 1851), the 1851 VIII MSK event was a seismic sequence that lasted more than 6 months (Table 2). Earthquakes felt on the island before the 1851 event occurred between 1827-1835, about 16-24 years before, with maximum intensities of VI MSK (IGN,1996) at Sineu and Palma.

The location of the macroseismal epicenter listed in the Spanish catalog (02.48.00E-39.36.00N) lies in the center of a circle joining Marratxí (nowadays Sa Cabaneta), St. Jordi and Sta. Eugènia (Pujó, 1851), where the strongest ground shaking was felt. Despite the inaccuracy of this determination, all the old reports (Bouvy, 1851; 1853; Pujó, 1851) agree that the macroseismal zone (VIII MSK) was located between Marratxí and Sta. Eugènia, about 11km NE of Palma (Fig. 1). This zone, located in the southern limb of the Sta. Eugènia antiform, coincides with the SW deflected prolongation of the Sencelles fault around the basin of Palma bay as suggested by Del Olmo and Alvaro (1984).

During the 1851 main shock, ground motion was felt in a zone of about 497 km^2, with a mean width of 13 km (Pujó, 1851), in the polygonal area defined by the towns of Sóller, Valldemossa and Banyalbufar in the Northwest and Palma, S'Arenal and Sencelles in the Southeast. This ground shaking distribution broadly coincides with the geometry of the Palma and Inca sedimentary basins and the adjacent mountainous sector of the Tramuntana range (Fig. 1).

In the macroseismal zone, most of the villages, such as Marratxí, Sta. Eugènia, and the formerly uninhabited districts of Sa Cabaneta and Portol suffered severe damage in some parts. At some distance from this zone, strong ground motion was felt in the West, at the villages located on the soft-sedimentary filling of Palma bay, especially at Sant Jordi and Palma (Pujó, 1851). But it was also felt, with high intensity at Sta. Maria del Camí, located at Inca basin, as reported by contemporary journals (El Heraldo, 1851; La Esperanza, 1851). At all these sites, seismic shaking was presumably amplified by ground conditions (soft sediments, high water table, etc.). From the descriptions available, seismic shaking in the Palma bay zone ranged from VII-VIII MSK intensity, causing moderate damage to buildings. Many towers and cupolas of churches collapsed in Palma, including those of the western wall of the Cathedral (Bouvy, 1851). The main buildings affected were the churches of Sta. Eulàlia, St. Miquel St. Francesc, St. Agustí, Concepció, Socor and the Montesión College, located in the old part of the town. Other administrative buildings such as, the post office, city hall, old market, the seat of the Military Governor, and fortifications suffered moderate damage (Diario Constitucional de Palma, 1851). Damage to the prison was considerable and some convicts were evacuated to military installations at Manacor (East of Mallorca), where the earthquake was felt only by some people (El Heraldo, 1851). Some cupolas and towers suffered inertial rotation of a maximum of 60º in Palma (Bouvy, 1951). Many houses and, especially church towers, were subsequently demolished to forestall further dangerous collapses (Diario Constitucional de Palma, 1851).

In the Tramuntana range, at Sóller, Valldemossa and Banyalbufar (in the NW of Mallorca) ground shaking (ranging from V to IV MSK intensity) triggered small to moderate rock-falls, and some clocks stopped (La Esperanza, 1851; Diario Constitucional de Palma, 1851), (Fig. 1). In the East, ground shaking was abruptly attenuated, following the line delineated by the Sencelles fault. Villages along this line (i.e. Sencelles) underwent intensities of V-IV MSK, whereas at other sites to the East/Southeast (i.e. Sineu, Manacor, Felanitx, and Campos) the earthquake was only felt with low intensities (III MSK, Fig. 1). At Campos, hot springs underwent overheating accompanied by an ejection of sulfur gas and muddy waters (Pujó, 1851). The earthquake was not felt at Artà, in the northeasternmost corner of the island, and there are no reliable data on Inca, Sa Pobla, Alcúdia and Pollença in the North of the island. The absence of news suggests that the ground motion was weak. By contrast, the ground motion was felt, with an intensity of III MSK, in the island of Cabrera, about 22 km South of Palma bay (Pujó, 1851). The first isoseismal map of the 1851 Palma event was drawn on the basis of these data. The geological nature of the ground, and terrain distribution should be taken into account for a more realistic interpretation (Fig. 1), showing a strong directivity of the ground motion, towards the WNW quadrant of the island. Moreover, soil (Palma bay) and topographic (Tramuntana range) factors probably amplified the ground shaking in this sector.

At least 13 earthquakes were felt in the macroseismal zone during the aftershock sequence (Galbis, 1932). Twenty days after the main event (7/6/1851), the main aftershock of at least intensity VI (Galbis, 1932) destroyed most of the previously damaged buildings, causing the total collapse of the Sant Marçal church at Marratxí and moderate ground

failures (Pujó, 1851). This second event represents a marked change in the characteristics of the seismic sequence (Table 2). During the first period (before the main aftershock) seismic events were moderate between intensities IV-V MSK, whereas during the second period (after the main aftershock) a monthly continuous activity was recorded until the end of the sequence on 22/12/1851 (Galbis, 1932), but with low intensities (<III MSK). After 4 months of seismic quiescence, the activity was renewed in May 1852 (Table 2). In this new period at least 4 different earthquakes were felt on the island. The period ended on August 8th, when a V MSK event was again felt at Palma bay (Galbis, 1932). After this last event no further earthquake was felt on the island until March 1859.

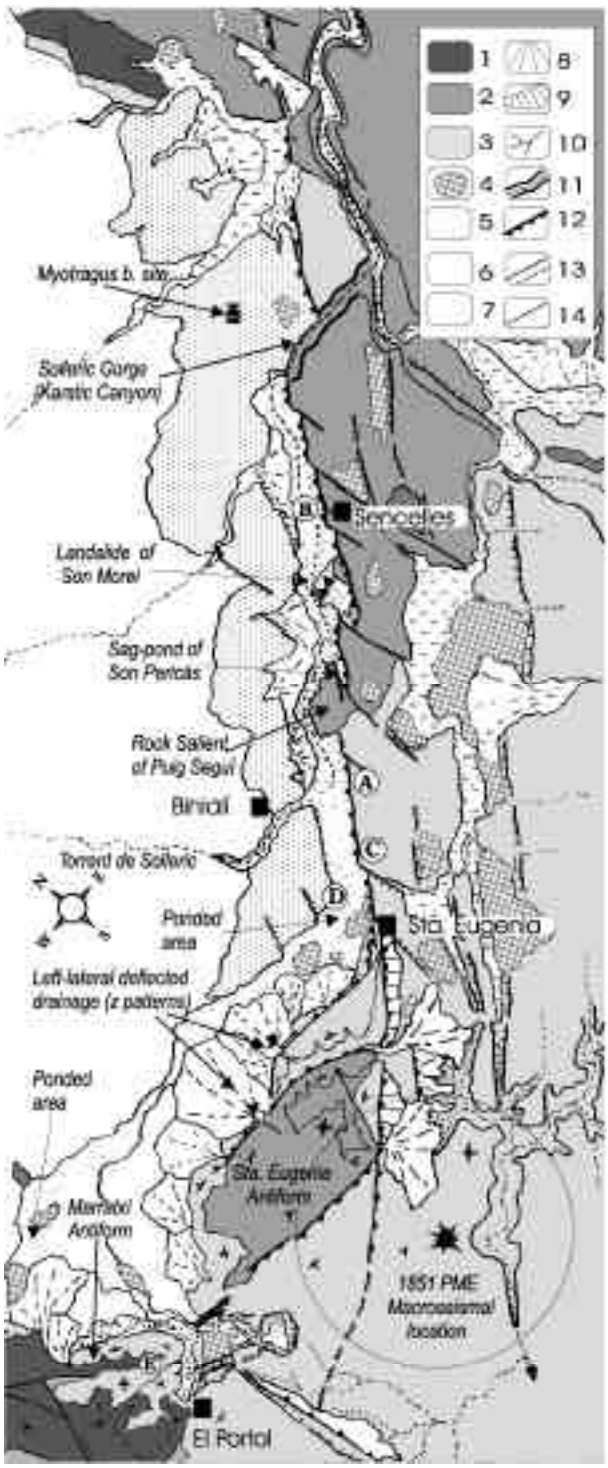

Finally, it should be pointed out that the macroseismal zone (Fig. 1) includes the areas of the island where recent surface ruptures, probably linked to the event, have been reported. These ruptures occurred along the main fault trace (Sta. Eugènia bedrock fault scarp: Silva et al., 2000) or along subsidiary structures (Portol doline reverse fault: Goy et al., 1991; Silva et al., 1999).

THE SENCELLES FAULT

The Sencelles fault (Fig. 3) constitutes the major extensional structure of the island with a clear surface expression. It generates the formation of the main

Figure 3. Schematic strip-map of the Sencelles fault showing its most prominent recent features. For location see Fig. 1. 1- Pre and syntectonic materials (pre-Serravallian); 2- post-tectonic pre-Pliocene materials (Serravallian to Messinian); 3- Plio-Quaternary materials (Fm. St. Jordi); 4- Quaternary dolines and ponded areas; 5- Pleistocene alluvial materials; 6- late Pleistocene to Holocene valley fillings; 7- late Pleistocene to Holocene alluvial fans; 8- colluviums; 9- drainage network; 10- karstic canyons; 11- normal fault scarps; 12- normal fault degraded scarps and erosive scarps. A, B and C: location of geological cross-sections of Fig. 4; D: location of surveyed zone of Figs. 5 and 6; E: location of the El Portol doline zone.

Figura 3. Mapa esquemático de la falla de Sencelles con indicación de las características recientes más sobresalientes. Situación en Fig. 1. 1- materiales pre y sintectónicos (preserravallienses); 2- materiales prepliocenos postectónicos (serravallienses a messinienses); 3- materiales pliocuaternarios (Fm. St. Jordi); 4- dolinas cuaternarias y áreas encharcadas; 5- materiales aluviales pleistocenos; 6- rellenos de valle tardipleistocenos a holocenos; 7- abanicos aluviales tardipleistocenos a holocenos; 8- depósitos coluviales; 9- red de drenaje; 10- cañones cársticos; 11- escarpes de falla normales; 12- escarpes de falla normales degradados y escarpes erosivos. A, B y C: situación de los cortes geológicos de la Fig. 4; D: situación de la zona explorada correspondiente a las Figs. 5 y 6; E: situación de la zona de la dolina del Portol.

tectonic landform of the island: a bedrock fault scarp approximately 7 km in length, running from Sencelles to Sta. Eugènia with a broad NE-SW orientation (N50°-60ºE), located on the calcarenites of the Plio-Quaternary St. Jordi Fm. (Pomar et al., 1983). Earlier geophysical data and bore-hole interpretations suggest that this structure extends to the NE (Alcúdia bay) and SW (Palma bay) covering a total length of 14 km (García Yagüe and Muntaner, 1968; Barón and González Casanovas, 1984; Benedicto et al., 1993). The fault scarp, facing to the NW, constitutes the southern border of the Inca basin and has been active since Serravallian times (Simó and Ramón, 1986). Gravity and seismic data indicate that this major fault has an accumulated throw of about 750 m (Benedicto et al., 1993), 100 m of which could have formed during Plio-Quaternary times as can be evidenced by available borehole data. The fault scarp height diminishes from 12 m near Sencelles to the SW to a few decimeters at Sta. Eugènia. On a broad scale, this linear tectonic landform gives rise to a tectonic valley (Torrent de Solleric) which runs parallel to the fault scarp (Fig. 3). To the NW a number of smooth asymmetric hills located on the older Quaternary materials of the Inca basin define the northern boundary of the valley (Fig. 3). These materials correspond to crusted alluvial fan sequences. They are slightly backtilted, displaying N55-75ºE strata orientations gently dipping to the NW (11º- 4º). Remains of *Myotragus balearicus* BATE (Cuerda, 1989) were found in these deposits (North of Sencelles). This endemic species provides a broad time-distribution with the result that these alluvial sequences can be assigned to a middle-late Pleistocene age.

The tectonic valley is occupied by the deflected NE-SW segment of the Torrent de Solleric, which drains into the Alcúdia bay through a well developed karstic canyon

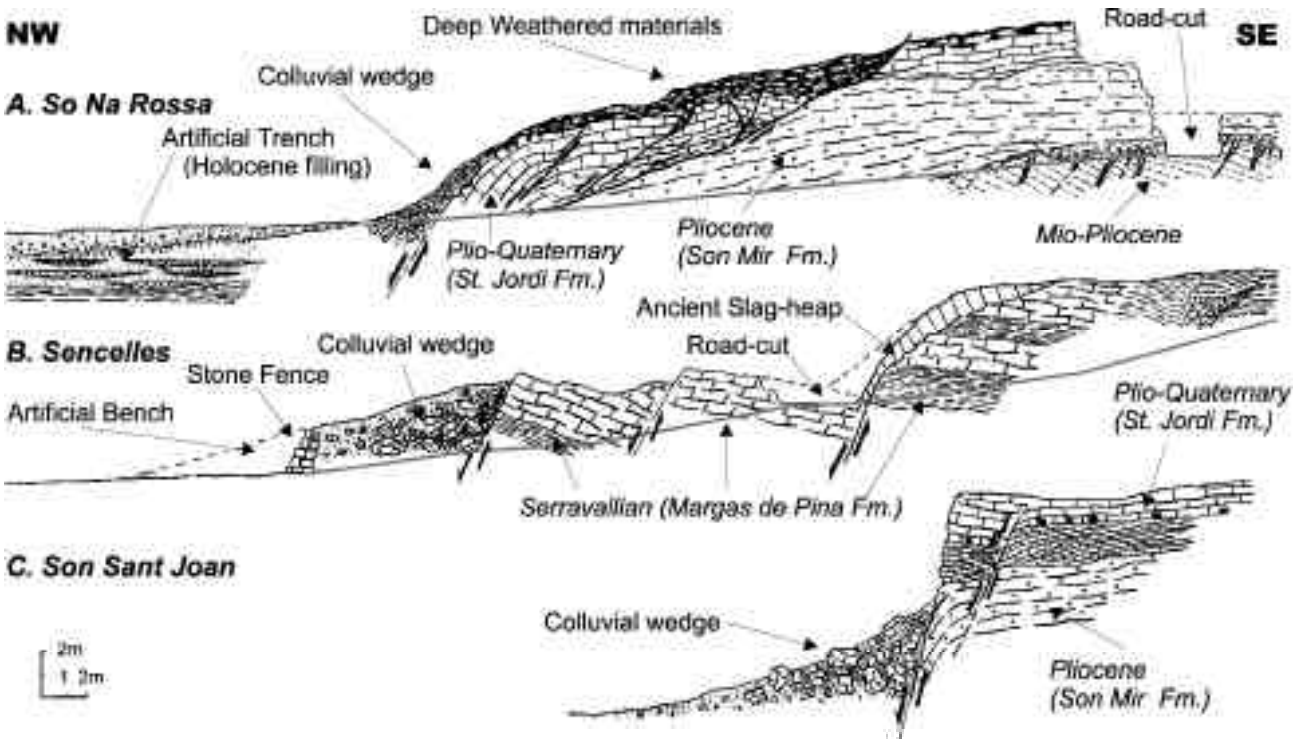

Figure 4. Geological cross-sections (scaled) along the Sencelles fault scarp showing the contrasting styles of extension based on the observed field data. A and C (Sta. Eugènia segment) on littoral Plio-Quaternary calcarenites of the St. Jordi Fm. with basal lower Pliocene calcareous silts (both) and marly deposits of theTerminal-Complex Fm. (A). B Sencelles segment on Serravallian limestones and laminated gypsy marls of the Margas de Pina Fm. For location see Fig. 3.

Figura 4. Cortes geológicos a lo largo del escarpe de la falla de Sencelles mostrando los distintos estilos extensionales, basados en datos de campo. A y C (segmento de Sta. Eugènia) en las calcarenitas pliocuaternarias de la Fm. de Sant Jordi con limos calcáreos del Plioceno inferior en la base (ambos) y depósitos margosos de la Formación del Complejo Terminal (A). B Segmento de Sencelles en las calizas serravallienses y las margas yesíferas laminadas de la Fm. Margas de Pina. Situación en Fig. 3.

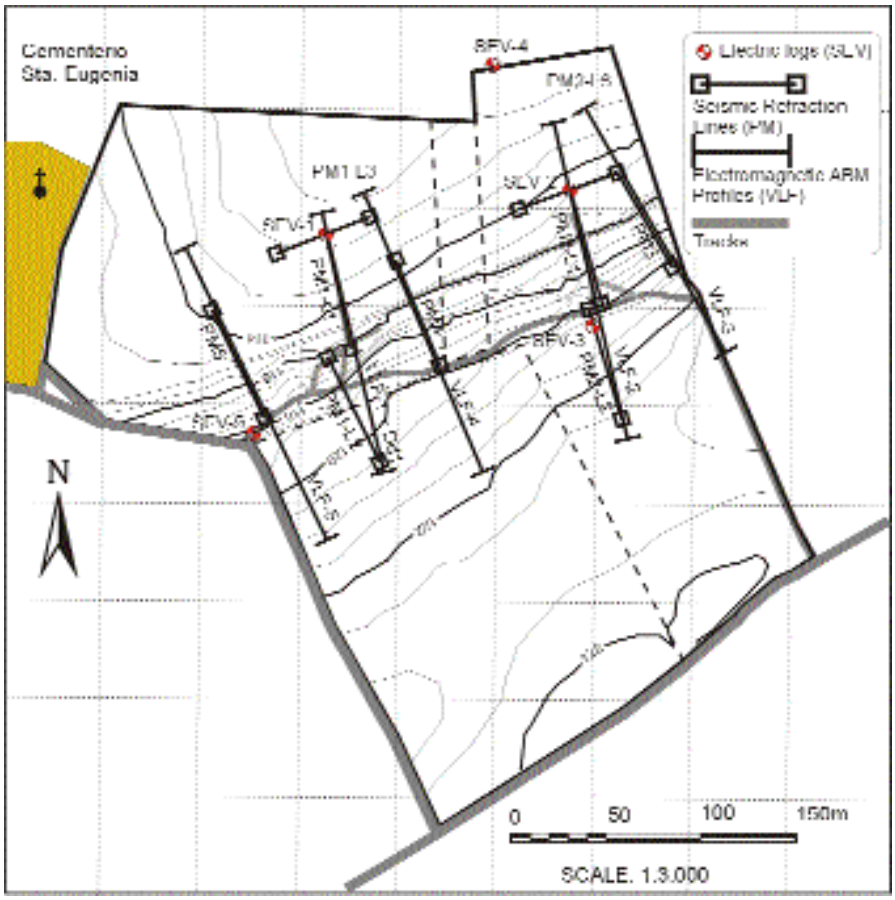

Figure 5. Topographic map of the surveyed zone at the Sta. Eugènia bedrock fault scarp. Geophysical survey-lines are also displayed and labeled. For location see Fig. 3.

Figura 5. Mapa topográfico del escarpe de falla de Sta. Eugènia. Se muestran las líneas de la campaña geofísica. Situación en Fig. 3.

NW of Sencelles (Fig. 3). The late Quaternary filling of the valley has a thickness ranging from 18 to 37 m. Dark levels rich in organic matter have been observed at the top of the sequences (Fuster and Barón, 1972). They were probably formed during earlier ponded stages by fault-related drainage damming prior to the presumably recent extrabasinal capture of the Torrent de Solleric. This was probably facilitated by the relevant sea-level drop documented offshore at the bays of Palma and Alcúdia (Díaz del Río et al., 1993) during the last glacial maximum. A large number of elongated, isolated dolines, and interconnected polje-type depressions control the poorly developed drainage network in the footwall to the South (Fig. 3). A NE-SW trending network of weakly incised karstic valleys captures the drainage from the Serres de Llevant, directing it to the bays of Alcúdia and Palma, through two lateral major karstic canyons that run parallel to the fault line.

Segmented nature of the Sencelles fault: structur al and g eomorpholo gic featur es

Fault geometry is characterized by the occurrence of two well defined segments, separated by a prominent rock salient (Puig Seguí) located on the older Serravallian deposits affected by the fault (Fig. 3). Rock highs are widely regarded as segment boundary diagnostic features associated with transverse faults and/or sharp lithological changes in normal fault range fronts (Wheeler, 1989; Machette et al., 1991). In our case, the main transverse fault is related to a poorly defined N10-20ºE normal fault on the eastern flank of the rock high, separating the Sta. Eugènia segment (West) and the Sencelles segment (East). The Sta. Eugènia segment consists of a simple bedrock fault scarp on highly indurate Plio-Quaternary calcarenites where minor transverse faults give rise to an en echelon arrangement of the fault (Fig. 3). By contrast,

the Sencelles segment has a more complex and higher fault scarp cutting through the older Serravallian materials. This scarp is characterized by subsidiary tectonic landforms such as, micro-graben depressions (Son Pericàs) and large old landslides (Son Morei), which complicates the fault geometry (Fig. 3).

Moreover, the fault scarp features vary from segment to segment, displaying different styles of extension (Fig. 4). The Sencelles segment is characterized by the main fault scarp located on calcareous and gypsiferous Seravallian materials. This scarp is heavily weathered and almost completely buried beneath massive colluvial wedges (Fig. 4B). By contrast, the Sta. Eugènia segment fault scarp corresponds to a limb-like fold scarp, probably controlled by rollovers at depth. The rollovers are characterized by warping and verticalization of littoral calcarenitic series which are eventually detached by more recent and discrete normal fault planes dipping NW. In the footwall, deformation is accommodated by the generation of subsidiary normal faults which eventually converge on a low angle horizon of detachment (Fig. 4A). The eventual fault scarps are sub-vertical, and the occurrence of isolated microrills enhance the orientation of former fault plane striations. To the East (Son Sant Joan; Fig. 4C) the formation of massive colluvial wedges, with boulder-sized blocks of calcarenites, completely or partially burying the bedrock scarp is common. However, to the West there is a single normal fault free-scarp, 3.5 to 0.1 m in height, which displays clear features of recent fault activation.

The Sencelles fault underwent a considerable change to the West of Sta. Eugènia. As evidenced by gravity and seismic data (Benedicto et al., 1993) the fault zone forks, flanking the two sides of the Sta. Eugènia antiform, which is regarded as an axially folded relief of a horst-like nature at depth (Fig. 3). The Serravallian gypsiferous materials (Margas de Pina Fm.) occupy, and probably intrude into the antiformal core. The late Neogene deposits (Tortonian-Pliocene) are arranged in a set of sharply dipping cuesta-type reliefs which are cut by the northern and southern branches of the Sencelles faults. The southern branch has a similar NE-SW orientation, but faces to the SW and is deflected towards Palma bay along the Son Sardina fault (García Yagüe and Muntaner, 1968; Silva et al., 1997). By contrast, the northern branch is deflected to the North, with a main NW-SE orientation (Benedicto et al., 1993). This branch also extends to the NW along the northern boundary of the Marratxí antiform. Several geomorphic anomalies such as discrete drainage deflections, bayonet patterns and stream beheadings are located along its trace, indicating the occurrence of a limited subsidiary left lateral slip during the recent Quaternary (Fig. 3).

Paleoseismic features in the w esternmost sector of the Sta. Eugènia segment

This sector displays a bedrock fault scarp on Plio-Quaternary calcarenites (St. Jordi Fm.). The height of this scarp diminishes from East to West, from ca. 3.5 m gradually petering out in the proximity of the Sta. Eugènia cemetery (Figs. 5 and 6). The footwall (South) is constituted by the aforementioned indurate calcarenites. They are gently warped, giving rise to moderate

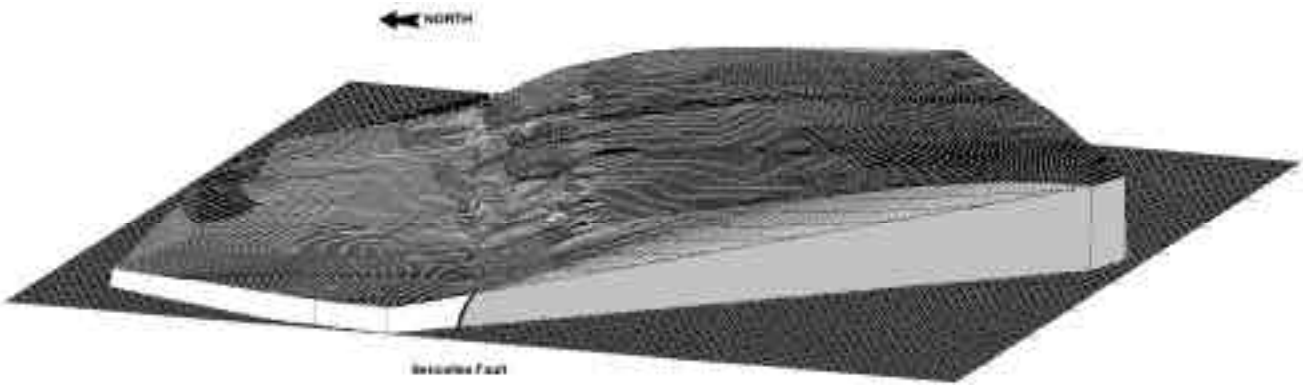

Figure 6. Digital elevation model of the surveyed zone in Fig. 5 (vertical exaggeration x3), showing the occurrence of the clear fault scarp on the surface.

Figura 6. Modelo digital del terreno del area de la Fig. 5 (exageración vertical x3) que muestra el neto escarpe de falla en superficie.

Figure 7. Detail of the two basal differentially weathered fault ribbons in the western sector of the Sta. Eugènia bedrock fault scarp (Sencelles fault). Hammer for scale is 33 cm long. Note that the hammer is within an artificial exploration scour 15 cm depth.

Figura 7. Detalle de las dos bandas basales, meteorizadas en distinto grado, en el sector occidental del escarpe de falla de Sta. Eugènia desarrollado en el sustrato (falla de Sencelles). El martillo utilizado como escala tiene una longitud de 33 cm. Nótese que el martillo se encuentra en un surco de exploración artificial de 15 cm de profundidad.

wavelength anti- and synformal structures, which is reflected on the surface topography (Fig. 6). With the exception of weathered horizons and thin veneers of very-limited reworked products, the calcarenites are not covered with sediments in the footwall. Artificial trenches dug in this sector (*Tiro al plato* trench) reveal that the calcarenitic strata are gently folded in a monocline close to the main fault plane in a manner similar to that observed in the East. Deformation of new strata occurs in the same outcrop, indicating the clear synsedimentary nature of this folding.

Differentially weathered ribbons on this rocky scarp (Fig. 7) along the easternmost 840 m of this fault segment provide evidence of recent reactivation. It may be assumed that this banding was produced during the most recent recurrent displacements of the fault in a manner similar to that generated on calcareous bedrock fault scarps during the 1981, 7.1 mb, Alkonides earthquake in the Aegean region (Mariolakos et al., 1998) and in the 1915, 7.5 mb, Pleasant valley earthquake in Nevada (Wallace, 1984). In the former case, a thin reddish pedogenic veneer stained the toe ribbon of the activated fault plane, whereas in the latter case a larger, differentially weathered, fault ribbon was formed.

In our case, no evidence of pedogenic veneer is present at the fault scarp toe. As indicated by Wallace (1984) and Stewart and Hancock (1989), this kind of pedogenic feature normally disappears after a few decades. The last reactivation of the Sencelles fault occurred during the 1851 Palma earthquake, about fifteen decades ago. A detailed study showed three differently weathered bands from scarp crest to toe. Moreover, different kinds of lichen colonies and varying degrees of lichen colonization observed by Wallace (1984) in the Pleasant valley can also be observed in these weathered ribbons.

An old upper band, 2.5 to 0.4 m wide, from East to West, is characterized by intense microkarstification, colonized by large black old groups (60-40 mm Ø) of lichens, covering the weathered fault plane. These lichens are overlapped by smaller yellow colonies (25-10 mm Ø) and by zones of more recent light-colored lichens (Fig. 7). A second band, 0.3 - 0.4 m wide, shows isolated but well developed microrills, and black lichens which are less dominant than the yellow ones, which cover most of the fault band. Finally, a third band, 0.15 - 0.2 m wide, with almost no karstification can be observed at the scarp toe. This band is characterized by the predominance of disperse spots of the most recent white lichen colonies (Fig. 7).

These differential weathering bands can be attributed to the most recent recurrent activity of the Sencelles fault on this segment, the lowest one having a very young appearance. Lichen identification, characterization, and a detailed analysis of lichenometry (lichen growth rates) are essential for a correct evaluation of faulting events, slip-rates and age bracketing. Lichenometric comparisons between fault plane colonies and similar lichen colonies observed on old gravestones and churches in the vicinity, made of similar Plio-Quaternary calcarenites could help

to date the paleoseismic events recorded on this fault segment. These comparative analyses of different 19th century gravestones and the scarp-toe band could be useful in accepting or rejecting the view that the last reactivation was caused by the 1851 earthquake. Based on the relative age of the faulted materials and the fresh morphology of the bedrock fault scarp, it is possible to affirm that the observed 3.5 m of displacement is Quaternary in age, and probably occurred in the last ca 10 ka. Similar banded fault planes in calcareous bedrock in the Mediterranean region have been interpreted as having formed during strong-magnitude (M_W>5.5) Holocene earthquakes (Armijo et al., 1992; Mariolakos et al., 1998; Michetti et al., 2000; Vittori et al., 2000).

By contrast, the hanging wall is made up of soft sediments, of a mainly clayey nature. These sediments were deposited in extensive but isolated palustrine zones fed by the alluvial systems of the Sta. Eugènia antiform and were located in the marginal headwater areas of the aforementioned tectonic valley (Fig. 3, Torrent de Solleric). As observed in the vicinity of Sencelles, these sediments often contain recent dark levels rich in organic matter suitable for radiocarbon dating. This area was, therefore, selected for a fault-trench analysis for the following reasons: weathering paleoseismic evidence, probable occurrence of suitable levels for dating and the fact that this sector is within the macroseismal zone of the 1851 Palma earthquake. A preliminary geophysical survey has been carried out in the selected zone (Silva et al., 2000) in an attempt to elaborate a fault trench project.

Geophysical survey of the Sta. Eugènia segment: the fault-trench project

The selected zone is located where the western fault peters out near Sta. Eugènia, and the fault scarp is dominated by the most recent band of weathering. A polygonal area of 200x400 m orthogonal to the fault scarp trace was surveyed and mapped at a scale of 1:5000. A grid of orthogonal lines and bench marks was positioned to insert the different geophysical lines (Fig. 8). Four techniques were used to collect information from the geophysical parameters: overlapping seismic refraction lines, VLF electromagnetic lines, electrical resistivity logs and single dipolar electrical lines. The methodology and preliminary results can be found in Silva et al. (2000).

Preliminary interpretations of the seismic profiles by simple 2-3 layer models show a buried fault-induced step

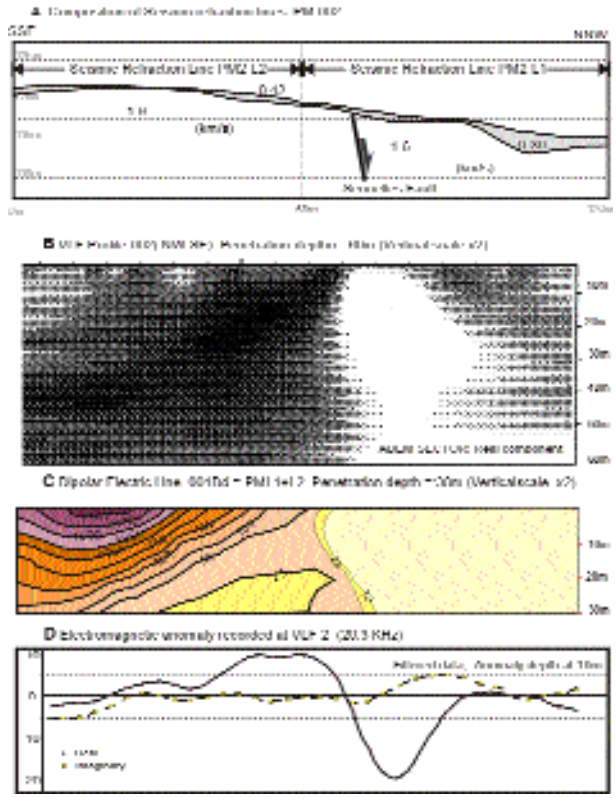

Figure 8. Preliminary interpretation of geophysical survey carried out at the Sta. Eugènia bedrock fault scarp. A: Interpretation of seismic refraction L1 and L2 lines of the PM2 array (see Fig. 5). B: Electromagnetic profile of line VLF2 at penetration depth of 60 m and vertical exaggeration x2. C: Dipolar electric profile of PM1 seismic line at penetration depth of 30 m and vertical exaggeration x2. D: Electromagnetic anomalies of the real and imaginary components of VLF2 line, filtered data for 20.3 KHz at 10 m depth.

Figura 8. Interpretaciones preliminares del estudio geofísico llevado a cabo en el escarpe de falla de Sta. Eugènia. A: Interpretación de las líneas de sísmica de refracción L1 y L2 del dispositivo PM2 (ver Fig. 5). B: Perfil electromagnético de la línea VLF2 con una profundidad de penetración de 60 m y una exageración vertical x2. C: Perfil eléctrico dipolar de la línea sísmica PM1 con una profundidad de penetración de 30 m y exageración vertical x2. D: Anomalías electromagnéticas de los componentes reales e imaginarios de la línea VLF2, datos filtrados para 20,3 KHz a una profundidad de 10 m.

displaced 10-15 m to the North of the surficial fault scarp (Fig. 8A). Fault throw related to this subsurface step progressively decreases from 5 to 1 m towards the NW in a manner similar to the surficial fault scarp. The recent soft-sedimentary materials burying this fault step have low velocities (Vp), such as 490 m/s, whereas the

suspected indurate calcarenitic substratum displays high velocities which can reach 1500 m/s. In the footwall a fine veneer (0.7 - 2 m thick) of weathered materials, mainly red clays, is clearly visible, showing velocities of about 400 m/s (Fig. 8A).

By contrast, resistivity log data indicate at least 3 different subsurface electric units in the hanging wall zone (Silva et al., 2000). For the correct interpretation of these units, it is necessary to take into account the presence of a saline aquifer (sulfate-rich water at 2.5 m depth) in the soft-sediment filling of the hanging wall sector as observed at nearby wells (Silva et al., 2000). The interpreted electrical units in the footwall are: 1) a thin upper unit (1.5-2.5 m thick) of recent detrital sediments with an apparent resistivity of 105-145 W/m; 2) a wedge-shaped middle unit, thickening to the North from 6-8 m to a maximum of 42 m over a distance of 90 m, which can be interpreted as old detrital materials and/or highly weathered calcarenites containing saline groundwater (6-4.3 W/m); and 3) a lower impermeable unit (944-675 W/m) probably made up of marls and/or calcareous silts.

Finally, the VLF-ABEM electromagnetic profiles show an abrupt lithological change in the fault plane (Figs. 8B and 8D). The fault plane appears as a subvertical feature slightly dipping to the North in keeping with its extensional nature. The hanging wall is characterized by a pronounced negative anomaly in the phase component (real), probably due to the presence of near surface low-penetrative materials, which in the complete ABEM profiles show dome-like and even fungiform geometries (Fig. 8B). These complex electromagnetic anomalies are also slightly displaced to the North of the fault trace near the sites where the seismic steps were recorded. The dipolar resistivity profile offers similar results. An abrupt resistivity drop down to 10 W/m is recorded along the suspected fault plane (Fig. 8C), and is also influenced by the saline water in the hanging wall sector.

Taken together, the geophysical data offer at least two interpretations involving evaporitic rocks. The area contains these rocks owing to the occurrence of sulfate-rich waters in neighboring wells and, indirectly owing to the abrupt resistivity drop recorded by both electrical logs and dipolar profiles. Given that no Messinian gypsums have been found on the island (Pomar et al., 1983; Alvaro et al., 1984), the only evaporitic materials accounting for these hydrological and geophysical features are the gypsums and gypsy marls of the Margas de Pina Fm. This sedimentary unit attains a thickness of up to 650-500 m in the Inca basin, (Pomar et al., 1983; Barón and González Casanovas, 1984; Gelabert, 1998). These authors relate the occurrence of the Margas de Pina Fm. to the dome and/or antiform-horst like geometries in different geological cross-sections based on core-drillings and seismic reflection lines. Moreover, these materials commonly appear in the inner part of the antiform-like structures (Marratxí and Sta. Eugènia antiforms), separating the basins of Inca and Palma (Del Olmo et al., 1991; Silva et al., 1997). This arrangement could be related to some kind of limited or assisted diapiric processes (Silva et al., 2000). These processes could account for the strong gravity anomaly (-13 mgal) of the sub-circular pattern in the SW corner of the Inca basin reported by Benedicto et al. (1993).

The geophysical anomaly could initially be interpreted as the result of near-surface diapiric processes, probably favored by fault activity. Another interpretation could be related to the use of the fault as a preferential zone of meteoric water infiltration, accelerating the dissolution of the suspected buried evaporitic materials at depth, and resulting in a local increase in groundwater salinity. The electromagnetic and electric results could be conditioned by this salinity rather than by fault geometry. The latter interpretation also demands evaporitic materials at shallow depth. In conclusion, the spatial coincidence of electromagnetic negative anomalies with the seismically recorded fault–related steps point to the occurrence of some kind of near-surface salt tectonics closely related to fault activity.

REVERSE FAULTING AT THE PORTOL DOLINE

The Portol doline is located between the NW-SE trending antiforms of Marratxí and Sta. Eugènia in the border zone of the Palma and Inca basins. Pliocene and early Pleistocene calcarenitic deposits of littoral and eolian origin are found in these two main structures (Del Olmo et al., 1991; Silva et al., 1997). In particular, at Marratxí, the present anticline-like pattern of the calcarenitic outcrops results from the superposition of: 1) late Pliocene littoral deposits folded in a monoclinal style by rollover-type extensional structures in the northern "limb" (Silva et al., 1997), and 2) Plio-Pleistocene eolian sediments gently dipping SW (towards the Palma bay) in the southern "limb". A similar situation can be inferred for the more complex antiform of Sta. Eugènia (Fig. 3), where diapiric processes could have favored its structure. Aside from

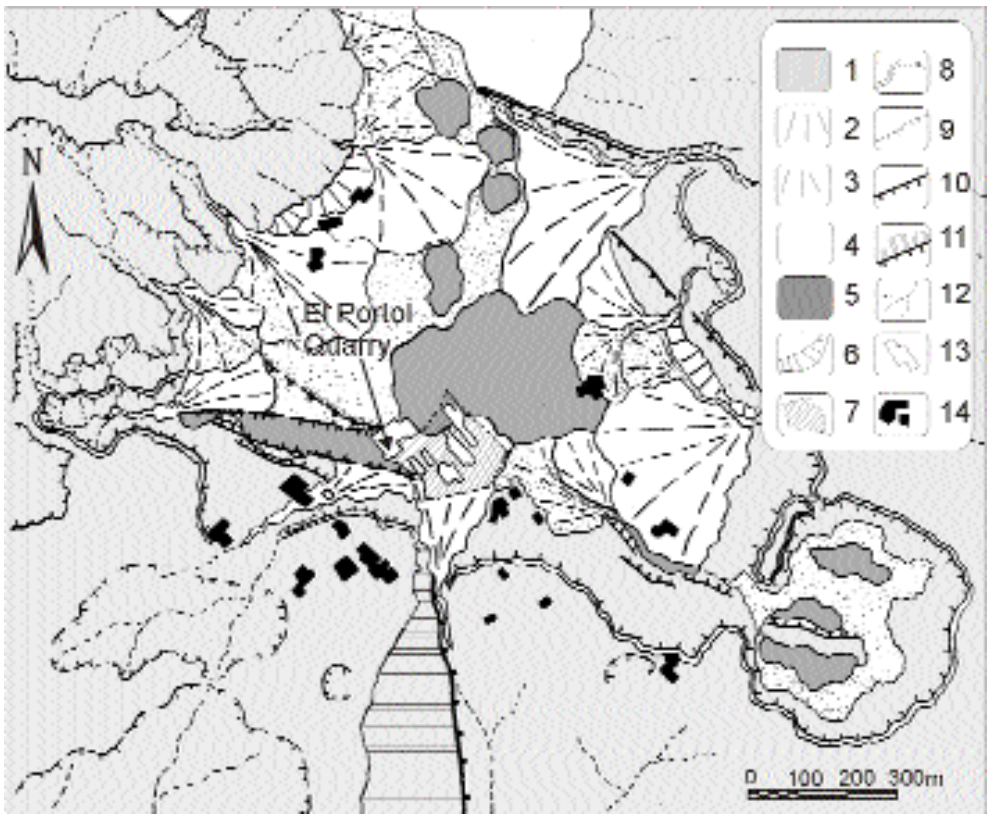

Figure 9. Detailed geological map of the Portol doline zone. 1- Plio-Quaternary calcarenites (substratum); 2- late Pleistocene-Holocene fans; 3- recent fan deposition; 4- recent polje filling; 5- dolines; 6- colluviums; 7- removed terrain (excavation works in quarries); 8- polje borders; 9- erosional scarps including cuesta relief; 10- fault scarps; 11- faceted fault planes; 12- drainage network; 13- old quarries; 14- houses.

Figura 9. Mapa geológico de detalle de la dolina de Portol. 1- calcarenitas pliocuaternarias (sustrato); 2- abanicos tardipleistoceno-holocenos; 3- deposición de abanicos recientes; 4- relleno de polje reciente; 5- dolinas; 6- depósitos coluviales; 7- tierras de acarreo (trabajos en canteras); 8- bordes de polje; 9- escarpes erosivos incluidos relieves en cuesta; 10- escarpes de falla; 11- planos de falla con facetas; 12- red de drenaje; 13- canteras antiguas; 14- casas.

the extensional and/or diapiric origin of these complex antiform structures (Portol doline), there is also some reverse surface faulting (Fig. 9) in the younger Quaternary doline filling (Goy et al., 1991).

In plan view, the present-day doline has a near-circular shape with a mean diameter of 0.4 km in a major polje-type depression. This is a NW-SE elongated karstic feature formed on the Pliocene calcarenitic substratum, and conditioned by normal N120-140E bedrock fault scarps at both margins (Fig. 9). There are at least eleven different dolines in this depression, displaying two different typologies: elongate marginal dolines and inner near-circular dolines. The marginal ones, which are mainly located along the southern border of the polje, are formed on the calcarenites, and display NW-SE elongate geometries, enhancing their structural control. By contrast, the inner dolines have characteristic near-circular geometries, and can be considered as "alluvial dolines" formed in the sedimentary filling of the karstic depression. This filling is mainly constituted by distal alluvial deposits from the antiformal reliefs surrounding the polje and by reworked decalcification red-clays. The development of reddish-gley paleosols and discrete calcareous palustrine levels are a characteristic feature of the whole sedimentary sequence. Only one of the dolines differs from the aforementioned ones. This is the biggest of the marginal dolines, and is controlled by a recent elongate small graben in the Quaternary sedimentary filling, bounded on the South by fault scarps in the Plio-Quaternary calcarenites (Fig. 9).

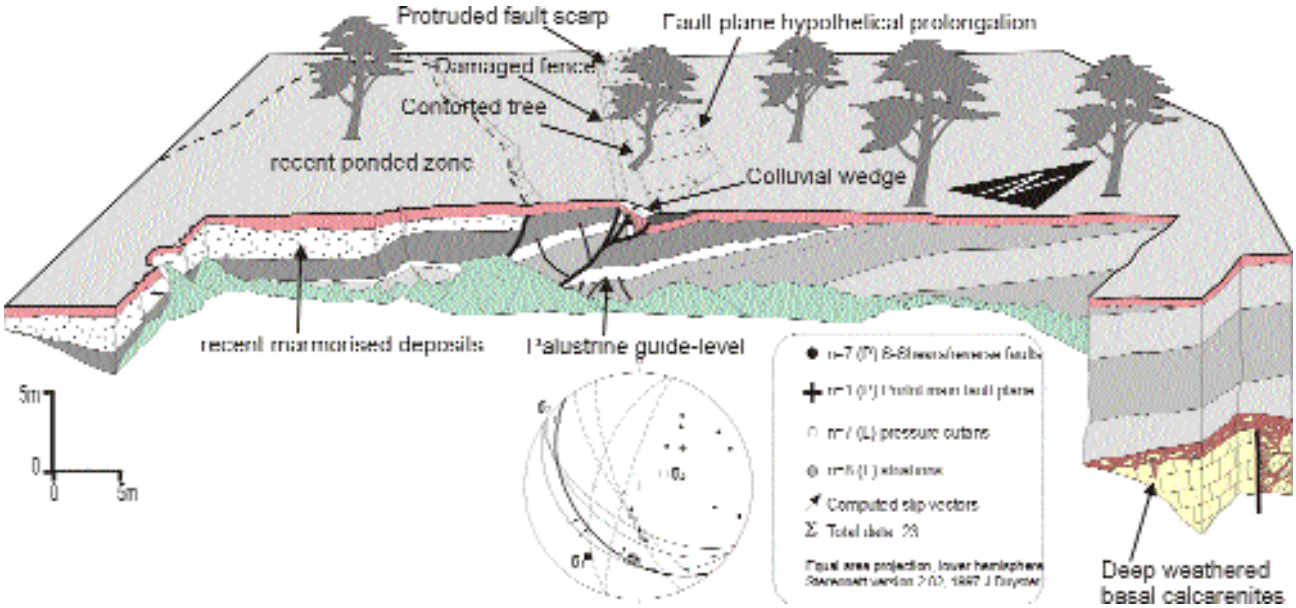

Figure 10. Block-diagram showing main deformational features displayed at the Portol doline reverse fault and stereoplot (lower hemisphere projection) of structural elements used for the determination of the main stress axis. In white, the palustrine guide level. Scaled gray strata represent the different alluvial inputs involved in the doline filling. In the right corner, basal deep-weathered calcarenite outcrop.

Figura 10. Bloque diagrama con las principales estructuras de deformación presentes en la falla inversa de la dolina de Portol y proyección estereográfica (hemisferio inferior) de los elementos estructurales utilizados para determinar el eje principal de esfuerzos. En blanco, el nivel guía palustre. Los estratos en distintos grises representan los distintos aportes aluviales al relleno de la dolina. En la esquina derecha, afloramiento de la calcarenita basal profundamente meteorizada.

Reverse faulting is evidenced in the walls of a quarry located in the southern sector of the biggest doline (Figs. 10 and 11), as reported by Goy et al. (1991). The doline filling (up to 20 m thick) is made up of a sequence of six different fine-grained distal alluvial inputs separated by reddish and/or brown paleosols, displaying well-developed gley features at thick Bt clayey horizons (0.2-0.6 m) in the uppermost part of each unit (Fig. 10). The presence of basal gravels in the different alluvial inputs, eroding and disrupting the underlying Bt horizons is also common. The basal deposits of the doline sequence are constituted by a thick unit (>5 m) of red sticky clays (*terra rossa*) which rest on the upper Pliocene littoral calcarenites. Large unweathered blocks of calcarenites occur within this basal unit, indicating its *in situ* weathered nature. The whole overlying Quaternary sequence is tilted 25º-20º SE, with a broad N30º-40ºE strata orientation.

Reverse faulting is highlighted by the offset of a calcareous palustrine level, 0.4-0.6 m thick, outcropping at the NW wall of the quarry. This quarry is an artificial trench which is 32.7 m in length and 2.3 to 11.8 m in depth. This outcrop allows the determination of good quality fault plane parameters. The vertical fault throw measured from the palustrine guide-level is 2.56 m, but the apparent total reverse slip of the up-thrusted segment measured along the fault plane is 5.20 m. The fault strikes N140º-130ºE, subparallel to the monoclinal fold axis of the adjacent Marratxí antiform, and dips towards the SW (N250º-240ºE). The fault dip is not uniform, and shows a variable angle which decreases upward, from 55º to 23º. In this convex geometry, sharp changes in the dip angle give rise to the occurrence of dip-slip restraining and releasing bends. The palustrine guide-level is disrupted in the upthrusted block, displaying a deformational style similar to that shown by fold-limb faults (Fig. 10). In particular, ground deformation resembles the coseismic low-angle pressure ridges along some sectors of the Spitak fault during the 1987 Armenian earthquake (Philip et al., 1992). Moreover, several sets of subsidiary normal and reverse faults, also dipping towards the SW, but oblique to the main fault (N150º-170ºE), display centimetric offsets (< 0.1m), accommodating the fault-

Figure 11. Picture of the reverse surface faulting at the Portol doline. Note surface disruption and contorted trees mentioned in text.

Figura 11. Fotografía de la falla inversa superficial en la dolina de Portol. Nótese la dislocación en superficie y los árboles torcidos mencionados en el texto.

induced dislocation in the upthrusted wall. A larger, normal oblique fault leads to an estimated displacement of up to 1.4 m in the upthrusted wall (Fig. 10). This last fault gives rise to the generation of the aforementioned small graben-type depression, in which the most recent Quaternary deposits are located (Fig. 9). These younger materials are massive red clays, displaying a wide range of pseudo-gley features, topped by a well-developed marmorized horizon, indicating the endorheic and restricted nature of the sedimentation (Silva et al., 1999). The whole faulted sequence is truncated by a thin alluvial veneer (0.4 to 0.6 m thick) of sandy clays which rest unconformably over the entire tilted doline sequence, constituting the present ground surface. This supports a recent and weakly developed brown soil which is also dislocated by the main fault plane (Fig. 10).

The fault consists of a fault gouge of about 4-12 cm in thickness in which the clayey sediments were deformed into a compact, firm and sheared, but locally brecciated, rock. Slickenside surfaces occur frequently within the deformed clays in subsidiary s-shears, but also on the footwall surface of the main fault plane, displaying striations and pressure cutans ranging from 90º to 122º SE pitch. From these kinematic elements Silva et al. (1999) re-calculated the net oblique slip of the upthrusted wall, giving an estimated value of ca. 5.58m. Conventional structural analysis performed in this study yielded a consistent N210º-220ºE orientation for the compressional stresses. Only some isolated data (internal s-shears) hold a more disperse distribution, indicating N274º-280ºE compressional stresses. This inconsistency in relation to the NW-SE extensional field governing the most recent evolution of the island is explained by the subsidiary synthetic character of the reverse faults in relation to the roll-over associated with the main normal faults along the polje border (Silva et al., 1999).

Surface faulting featur es

Ground surface dislocation is recorded by the occurrence of a reverse fault scarp dipping to the NE, opposite the SW fault dip, which ranges in height from 0.88-0.20 m along the up-thrusted segment (Figs. 10 and 11). Fault scarp morphology can be classified as a protruded scarp (Gordon and Lewis, 1980) in which the palustrine guide level folded, and collapsed, resulting in a breccia. The scarp front is partially buried. A colluvial wedge with a slope of 27º connects both fault blocks. This includes large calcarenitic blocks (40x20 cm) of a severely damaged old stone wall. The fault scarp crest strikes N158º-163ºE in a manner similar to the subsidiary reverse faults located in the upthrusted block, and the fault scarp toe strikes following the mean orientation of the main fault (N140ºE). Further to the NW, these two geomorphic elements of the fault scarp tend to converge inducing the progressive decrease in the height of the fault scarp from 0.88 to 0.20m (Fig. 10). The fault scarp dies out abruptly at a transverse stone wall, 197 m away from the quarry, which does not correspond to the original true fault scarp termination. Simple trigonometric relationships based on the present geometry of the different fault planes involved allowed us to estimate an original fault scarp-length of ca. 535 m towards the NW. To the SE, ground movements caused by former quarry excavations have also destroyed the fault scarp (Fig. 9). Moreover, the south wall of the quarry opposite the fault outcrop is currently covered with a slag-heap. Despite these factors, levelling of the ground surface southwards of the present quarry shows a mean dislocation of ca. 1.20 m. This suggests a prolongation of the fault scarp over the ca. 120 m separating the quarry from the polje border. Reverse surface faulting seems to be confined to the softer sediments of the doline with a maximum rupture length of ca. 650 m (Fig. 9).

Age of probable faulting ev ents

Paleomagnetic surveys carried out in the sedimentary sequence of the doline (Goy et al., 1991; González Hernández, in prep.) indicate a constant normal polarity

in all the different sedimentary units. Based on the Quaternary age of the deposits, the whole sequence has been attributed to the Brunhes epoch, and therefore to an age younger than 0.78 Ma. (middle Pleistocene onset). Although the absence of more than one guide-level does not facilitate an accurate fault history, the present outcrop allowed us to infer a complex multi-event history. The contrasting values of displacement shown by the fault throw (2.56 m) and the present surface faulting ground dislocation (0.88 m) suggest at least two different periods of activity: 1) a major period of seismic events (middle to late Pleistocene) during which at least 1.68 m of fault throw accumulated; and 2) a more recent Holocene period during which a maximum ground vertical dislocation of 0.88 m was produced along the present fault scarp. Given that the maximum estimated values of the surface rupture length (ca. 650 m) and the maximum displacement (ca. 0.88 m) do not match the empirical relationships proposed by Wells and Coppersmith (1994), the fault scarp probably records a multi-event history.

The very recent paleoseismic activity along this fault scarp is characterized by three main features. 1) An old stone wall striking along the fault scarp is severely damaged and large calcarenitic stones from the wall are included in the fault scarp-related colluvial wedge. 2) Some of the old and unproductive almond trees located on the fault scarp are strongly tilted towards the NE reaching inclinations of up to 40º (Figs. 10 and 11). In all the cases, the tree trunk inclinations occurred during early growth given that the orientation of the tree trunks changes abruptly from an inclined position to a vertical one close to the base (Fig. 11). This accounts for the occurrence of contorted trees only along the present fault scarp. 3) Some remains of the former herbaceous grass mat covering the ground surface of the footwall are buried beneath the colluvial wedge, highlighting the recent character of the surface disruption.

According to the quarry owners the present fault scarp morphology, the damaged stone-wall and the contorted trees existed before commencing quarry excavations in 1930. This zone of the doline has traditionally been used for clay extraction for the local pottery industry since the late 19th Century. Thus, the last deformation event occurred before 1930, probably in the 19th Century during the 1851 Palma seismic event as suggested by Silva et al. (1999). Further studies on surface disruption dating are warranted to attribute the reported deformations to the 1851 Palma event. Dendro-chronological analysis of the contorted tree-trunks could help in this task.

CONCLUSIONS

Mallorca is subject to low seismic activity. This activity seems to be confined to the upper brittle crust, where detachment-driven normal faulting processes have been characteristic for the last 12 Ma as has been pointed out by recent large scale seismic reflection profiling and gravity surveys (Benedicto et al., 1993; Sàbat et al., 1995; Gelabert, 1998). Only three major seismic events (≥ VII MSK) have been reported: in 1660, 1721 and 1851 (Galbis, 1932; IGN, 1996). The last event, known as the 1851 Palma earthquake (VIII MSK), can be described as a seismic sequence of at least 7 months' duration, initiated by the main shock on 15 May 1851, terminating on 12 December 1851 as documented by contemporary reports. The macroseismal zone is located between Marratxí (Sa Cabaneta) and Sta. Eugènia, to the South of the Sta. Eugènia antiform and close to the trace of the Sencelles fault. Moderate ground failure processes have been reported in the macroseismal zone during this seismic sequence (Pujó, 1851), including ground cracks, displacements and discrete rock falls. Outside this zone, ground shaking was mainly directed towards Palma bay, where the VIII-VII MSK shaking (Fig. 1) was presumably amplified by ground conditions (thick soft-sediment cover and high water table). However, the earthquake was weakly felt (III to II MSK) at similar distances from the macroseismal epicenter in the SE of the island.

Even in regions of moderate to low seismicity, prominent Quaternary fault scarps provide clear evidence for strong events. This has been documented in the Basin and Range area before the 1983 Ms 7.3 Borah Peak earthquake (Crone and Haller, 1991), in central Italy (Vittori et al., 2000), or even in currently aseismic zones like the Pollino region in southern Italy (Michetti et al., 1997, 2000) or in the Catalan Coastal ranges in northeastern Spain (Masana, 1996). Thus geological data could offer a more reliable means of identifying potentially hazardous faults than seismological data alone. This seems to be the case of the Sencelles fault, where there is clear evidence of recent activity. Two main zones were surveyed: the Portol doline and the Sta. Eugènia bedrock fault scarp.

Reverse surface faulting occurred at the Portol doline, generating a protruded fault scarp of 0.88 m in height similar to the coseismic low-angle pressure ridges reported in the Spitak fault (Philip et al., 1992). Reverse faulting records an accumulated throw of 2.56 m for, at least, the last 780 ka, as evidenced by paleomagnetic analyses. Apparent displacements per event range from

1.68 to 0.88 m (Silva et al., 1999). Given the disagreement between these displacement values and the values estimated from the surface rupture length (650 m), it can be assumed that the displacement was obtained during a multi-event fault history. This anomalous compressional feature cannot be considered as true surface faulting, but as a secondary or sympathetic surface faulting of Serva's classification (1993). This was probably caused by near surface roll-over processes along the major extensional faults bordering the southern margin of the polje-depression or by karstic ground failure promoted by seismic shaking.

On the Sencelles fault, recent faulting is recorded in the western part of the Sta. Eugènia segment. The maximum accumulated Quaternary surface dislocation recorded by the bedrock fault scarp on the indurate Plio-Quaternary calcarenites of the St. Jordi Fm. ranges from 3.5 to 4 m. This scarp displays diverse bands of weathering, which are colonized by young lichens in the lower bands and older lichens in the upper bands. This resembles the weathered bands recorded on other calcareous bedrock fault scarps (Mariolakos et al., 1998; Wallace, 1984). The preliminary analysis of the differentially weathered fault-ribbons sequence suggests the occurrence of discrete displacements per event ranging from 0.4 to 0.15 m.

Based on the evidence of damaged stone walls, contorted trees, lichen free scarp-toes, absence of pedogenic veneers, recent soil and dead grass mats buried by fault scarp collapse, etc., the most recent displacement has a historical character, probably related to the 1851 Palma earthquake (Silva et al., 1999; 2000). Further studies on dendrochronology and pedology at the Portol doline, and on lichenometry and weathering on the Sta Eugènia bedrock fault scarp are warranted not only for a correct evaluation of faulting event slip-rates and age bracketing but also for a reliable correlation of these events with the 1851 event. Simple empirical relationships proposed by Serva (1993) and Wells and Coppersmith (1994) indicate that the surface rupture length (SRL) is probably related to seismic events ≤ 4.9 M_W. This could only account for maximum vertical displacements (MVD) down to 5 cm which are lower than those observed (88 to 15 cm) at the Portol doline and Sencelles fault. Recent VII-VIII MSK earthquakes in Italy, (e.g. the 1997 Umbria-Marche (M_W =5.7) or the 1998 Lauria (M_W=5.6) events), showed maximum vertical displacements down to 8 cm on segments ranging from 0.3 to 1.8 km in length (Michetti et al., 2000; Vittori et al., 2000). Therefore, the disagreement between the predicted and observed SRL and MVD values reported in this work could be attributed to:

A) a more complex multi-event history than that inferred by the apparent maximum vertical displacement per event with the result that the island was affected by larger historical and/or prehistorical earthquakes before 1654 (onset of the Spanish seismic catalog);

B) the amplification of the vertical displacement due to karstic or diapiric processes favored by seismic shaking during individual events as suggested by the geophysical data obtained;

C) the secondary character of the coseismic ground failure observed as seems to be the case of the Portol doline (Silva et al., 1999).

In order to solve these uncertainties and to obtain a more complete paleoseismic record, a fault-trench analysis was planned at the western end of the Sencelles fault (Sta. Eugènia segment). A detailed topographic, geologic and geophysical survey was carried out in a selected zone of 200x400 m (Silva et al., 2000). Preliminary geophysical data indicate the occurrence of a subvertical fault plane dipping 80º-70º NW, and the development of a near surface fault-like step to the North of the fault scarp ranging from 5 to 1 m in height. VLF and electric data suggest the occurrence of near-surface diapiric processes, enhancing the subsurface deformation in the hanging wall. If confirmed, this could complicate the trench interpretation. The selected zone offers good possibilities for the excavation of a fault trench. There is, at least, a 5 m thick recent sedimentary cover in the hanging wall, and there is no evidence of indurate calcrete horizons that could complicate the excavation. Moreover, datable material (organic-matter bedding) is probably present.

Finally, it should be pointed out that given the absence of research on seismic hazard on the island, past destructive earthquakes warrant study. According to the present Spanish seismic code (NCS-94) expected maximum horizontal accelerations (basic ground acceleration) are 0.04 g for a 500 year return model. However, the available seismic data indicate the occurrence of VII-VIII MSK intensity events with shorter elapsed times of 61 to 130 years. Basic empirical relationships (Bolt, 1993; Keller and Pinter, 1996) show that VII to VIII intensities are normally related to potentially hazardous peak ground accelerations of up to

0.10 g, which could be amplified in the littoral sector of Palma bay as in the case of the 1851 event.

It is reasonable to assume that sufficient elastic energy has accumulated along the Sencelles fault since 1851 to be released in a new destructive event ($I_{max} \geq$ VIII). Recurrence intervals (I=III-IV) apparently related to the Sencelles fault range between 70-90 years. There is little doubt that the 0.04 g assigned by the Spanish seismic code (NCS-94) to Mallorca should be revised. This is an underestimated value which contrasts with the historical and geological data. Despite the few data available, the Palma bay basin and in particular its littoral sector (including the town of Palma) appear to constitute the most hazardous zone of the island as evidenced by the 1851 seismic sequence. This situation has been aggravated by the lack of research on paleoseismicity and seismic hazard on the island. Apart from the contemporary reports of Bouvy (1851; 1853) and Pujó (1851) compiled and summarized by Galbis (1932), and the works of Silva et al., (1999; 2000), the only published seismological contribution has been the isoseismal map corresponding to the V MSK 1964 Montuiri earthquake (Mezcua, 1982).

ACKNOWLEDGEMENTS

This work was supported by the Spanish DGES Projects PB98-0265 (Univ. Salamanca) and PB98-0514 (MNCCN, CSIC). The authors wish to thank Jesús Rodríguez Izquierdo (Biblioteca Nacional de Madrid), who facilitated documentation, and the City-hall councils of Sta. Eugènia and Sencelles for collaborating during field research. The comments and suggestions of Drs. A.M. Michetti and P. Alfaro contributed to the improvement of the final version of this paper.

REFERENCES

Alvaro, M., 1987. La tectónica de cabalgamientos de la Sierra Norte de Mallorca (islas Baleares). Bol. Geol. y Min., 98, 34-41.

Alvaro, M., Barnolas, A., Del Olmo, P., Ramírez del Pozo, J., Simó, A., 1984. El Neógeno de Mallorca: Caracterización sedimentológica y bioestratigráfica. Bol. Geol. y Min., 95, 3-25.

Armijo, R., Lyon-Caen, H., Papanastassiou, X., 1992. East-West extension and Holocene fault scarps in the Hellenic arc. Geology, 20, 491-494.

Barón, A., González Casanovas, C., 1984. Distribución espacial del Mio-Plioceno en la isla de Mallorca. Actas I Cong. Geol. Esp., 1, 137-148.

Benedicto, A., Ramos, E., Casas, A., Sàbat, F., Barón, A., 1993. Evolución tectosedimentaria de la cubeta neógena de Inca (Mallorca). Rev. Soc. Geol. España, 6, 167-176.

Bolt, B.A., 1993. Earthquakes. New York, W.H. Freeman and Co., 3rd ed., 331 p.

Bosi, C., Galadini, F., Messina, P., 1993. Neotectonic significance of bedrock fault scarps: case studies from the Lazio-Abruzzi Apennines (Central Italy). Z. Geomorph. N.F. Suppl. Bd., 94, 187-206.

Bouvy, P., 1851. Sobre el Terremoto ocurrido en la Isla de Mallorca el 15 de mayo último. Rev. Minera, 2(26), 375-378.

Bouvy, P., 1853. Notice sur le tremblement de terre du 15 mai 1851, de l'île de Majorque. Bol. Soc. géol. France, 10, 359-364.

Crone, A.J., Haller, K.M., 1991. Segmentation and the coseismic behaviour of Basin and Range normal faults, examples from eastern Idaho and southwestern Montana, USA. J. Struct. Geol., 13, 151-164.

Cuerda, J., 1989. El Cuaternario de las islas Baleares. Palma de Mallorca, Inst. Estudios Baleáricos, 409 p.

Dañobeitia, J.J., Arguedas, M., Ganyant, J., Banda, E., Markis, J., 1992. Deep crustal configuration of the Valencia trough and its Iberian and Balearic borders from extensive refraction and wide-angle reflection seismic profiling. Tectonophysics, 203, 37-55.

Del Olmo, P., Alvaro, M., 1984. Los sistemas de fracturación post-orogénicos de la Isla de Mallorca. Actas I Cong. Geol. Esp., 1, 137-148.

Del Olmo, P., Alvaro, M., Ramírez del Pozo, J., Aguilar, M.J., 1991. Mapa Geológico de España, scale 1:50,000, 2nd series, nº 698/723-IV, Palma de Mallorca. Madrid, IGME, Serv. Publ. Ministerio de Industria, 64 p., 1 fold. map.

Diario Constitucional de Palma, 1851. Suplemento del 15 de Mayo de 1851. Rev 469 Hemeroteca, Biblioteca Nacional de Madrid.

Díaz del Río, V., Somoza, L., Goy, J.L., Zazo, C., Rey, J., Hernández Molina, J., Mateu, G., 1993. Estudio fisiográfico de las bahías de Palma y Alcudia (Mallorca, España). Bol. Geol. y Min., 158, 123-149.

El Heraldo, 1850/51. Revmicro 170, Micro 19401. Hemeroteca, Biblioteca Nacional de Madrid.

Esposito, E., Porfido, S., Mastrolorenzo, G., Nikonov, A., Serva, L., 1997. Brief review and preliminary proposal for the use of ground effects in the Macroseismic Intensity assessment. In Y. Hong (ed.), Proc. 30th Int. Geol. Congr., Vol. 5, Tokio, Japan, 233-243.

Fontboté, J.M., Guimerà, J., Roca, E., Sàbat, F., Santanach, P., Fernández-Ortigosa, F., 1990. The Cenozoic evolution of the València trough (Western Mediterranean). Rev. Soc. Geol. Esp., 3, 249-259.

Fuster, J., Barón, A., 1972. Informe Hidrogeológico del Llano de Inca, Madrid, SGOP, 2 tomos.

Galbis, J., 1932. Catálogo Sísmico de la zona comprendida entre los meridianos 5ºE y 20ºW de Greenwich y los paralelos 45º y 25ºN. Inst. Geográfico, Catastral y de Estadística de España, Tomo I, 99-100.

García Yagüe, A., Muntaner, A., 1968. Estudio Hidrogeológico del Llano de Palma, Madrid, SGOP, 2 tomos.

Gelabert, B., 1998. La estructura geológica de la mitad occidental de la isla de Mallorca. I.T.G.E., Colección Memorias, 129 p.

Gelabert, B., Sàbat, F., Rodríguez-Perea, A., 1992. A structural outline of the Serra de Tramuntana of Mallorca (Balearic Islands). Tectonophysics, 203, 167-183.

Gordon, R.G., Lewis, J.D., 1980. The Meckering and Calingiri earthquakes October 1968 and March 1970. Geol Surv. West. Austral. Bull., 126, 229 p.

Goy, J.L., Zazo, C., Mörner, N.A., 1991. Reverse fault in continental sedimentary deposits on Mallorca. Abstract Vol., XIII Int. INQUA Congress, Beijing (China), p.118.

IGN, 1996. Catálogo Sísmico de España. Servicio de Sismología, Instituto Geográfico Nacional, Petición de datos nº 96/0001.

Keller, E.A., Pinter, N., 1996. Active Tectonics, Earthquakes, Uplift and Landscape. Upper Saddle River, New Jersey, Prentice-Hall Inc., 338 p.

La Esperanza, 1851. Revmicro 140, Micro 16455. Hemeroteca, Biblioteca Nacional de Madrid.

Machette, M.N., Personius, S.F., Nelson, A.R., Schwartz, D.P., Lund, W.R., 1991. The Wasatch fault zone, Utah -segmentation and history of the Holocene earthquakes. J. Struct. Geol., 13, 137-149.

Mariolakos, I., Fountoulis, I., Kranis, H., 1998. Formalization of Neotectonic Maps. Field Trip guide-book: Peloponessos-Sterea Hellas. 8th Int. Cong. Geol. Soc. Greece. Patra (Greece), 74 p.

Masana, E., 1996. Evidence for past earthquakes in an area of low historical seismicity: the Catalan Coastal ranges, NE Spain. Annali di Geofisica, 39(3), 689-704.

Mezcua, J., 1982. Catálogo General de isosistas de la Península Ibérica, Madrid, IGN, 322 p.

Michetti, A.M., Ferreli, L., Serva, L., Vittori, E., 1997. Geological evidence for strong historical earthquakes in an "aseismic" region: The Pollino case (southern Italy). J. Geodynamics, 24(1-4), 67-86.

Michetti, A.M., Ferreli, L., Esposito, E., Porfido, S., Blumetti, A.M., Vittori, E., Serva, L., Roberts, G.P., 2000. Ground effects during the 9 September 1998, Mw=5.6, Lauria Earthquake and the seismic potential of the "aseismic" Pollino Region in southern Italy. Seismological Res. Lett., 71(1), 31-46.

NCS94, 1996. Norma de Construcción Sismorresistente: Parte General y Edificación. In Norma Básica de la Edificación NBE AE-88, Serie Normativas, Madrid, Ministerio de Fomento, 79-135.

Philip, H., Rogozhin, F., Cisternas, A., Bousquet, J.C., Borisov, B., Karakhanian, A., 1992. The Armenian Earthquake of 1988 December 7: Faulting and folding, neotectonics and paleoseismicity. Geophys. J. Int., 110, 141-158.

Pomar, L., Marzo, M., Barón, A., 1983. El Terciario de Mallorca. In L. Pomar, A. Orador, J.J. Fornós, A. Rodríguez-Perea (eds.), El Terciario de las Baleares (Mallorca-Menorca), Palma de Mallorca, Inst. Est. Baleáricos, 21-45.

Pujó, M., 1851. Le tremblement de terre du 15 mai 1851 de l'île de Majorque. Comp. Rend. Acad. Sci. Paris, 2, 23.

Sàbat, F., Muñoz, J.A., Santanach, P., 1988. Transversal and oblique structures at the serres de Llevant thrust belt (Mallorca Island). Geol. Rundsch., 77(2), 529-538.

Sàbat, F., Roca, E., Muñoz, J.A., Vergés, J., Santanach, P., Sans, M., Masana, E., Estévez, A., Santiesteban, C., 1995. Extension and compression in the evolution of the eastern margin of Iberia: the ESCI-València Trough seismic profile. In P. Santanach (ed.), ECSCI – Estudios Sísmicos de la Corteza Ibérica, Rev. Soc. Geol. España, 8(4), 431-448.

Serva, L., 1993. An analysis of the world regulatory guides for nuclear power plant seismic design. Energia Nucleare, 2, 77-96.

Silva, P.G., González-Hernández, F.M., Goy, J.L., Zazo, C., 1997. Origen y desmantelamiento del Antiforme Plio-Cuaternario de Marratxí (Mallorca, España). Geogaceta, 22, 143-147.

Silva, P.G., González-Hernández, F.M., Goy, J.L., Zazo, C., Mörner, 1999. Quaternary reverse surface faulting in Mallorca Island (Baleares, Spain). Geogaceta, 26, 99-102.

Silva, P.G., Carrasco, P., González Hernández, F.M., Goy, J.L., Zazo, C., Luque, L., Santos, G., Delgado, M., Poza, L.J., 2000. Prospección geofísica de la Falla de Sencelles (Mallorca, España): Una metodología preliminar para la realización de trincheras de falla. Geotemas, 1(4), 359-363.

Simó, A., Ramón, X., 1986. Análisis sedimentológico y descripción de las secuencias deposicionales del Neógeno post-orogénico de Mallorca. Bol. Geol. Min., 157, 445-472.

Stewart, I., Hancock, P.L., 1991. What is a fault scarp? Episodes, 13(4), 256-263.

Vittori, E., Deiana, G., Esposito, E., Ferreli, L., Marchegiani, L., Mastrolorenzo, G., Michetti, A.M., Porfido, S., Serva, L., Simonelli, A.L., Tondi, E., 2000. Ground effects and surface faulting in the September-October 1997 Umbria-Marche (Central Italy) seismic sequence. J. Geodynamics, 29, 535-564.

Wallace, R.E., 1984. Fault scarps formed during the earthquake of October 2, 1951, in Pleasant Valley, Nevada, and some tectonic implications. U.S. Geol. Surv. Prof. Paper, 1274-A, 33 p.

Wells, D.L., Coppersmith, K.J., (1994). New empirical relationships among magnitude, rupture length, rupture width, rupture area, and surface displacement. Bull. Seism. Soc. Am., 84, 974-1002.

Wheeler, R.L., 1989. Persistent segment boundaries on Basin and Range normal faults. In D.P. Schwartz, R.H. Sibson (eds.), Fault segmentation and controls on rupture initiation and termination, U.S. Geol. Surv. Open-file Rep., 89-315, 432-444.